Progress in Pediatric Cardiology 54 (2019) 101128

Contents lists available at ScienceDirect

Progress in Pediatric Cardiology

journal homepage: www.elsevier.com/locate/ppedcard

Review

Novel insights into the genetic landscape of congenital heart disease with systems genetics

George C. Gabriel, Cecilia W. Lo*

Department of Developmental Biology, University of Pittsburgh School of Medicine, Pittsburgh, PA 15201, United States of America

A B S T R A C T

We recently conducted a large-scale mouse mutagenesis screen and uncovered a central role for cilia in the pathogenesis of congenital heart disease (CHD). Though our screen was phenotype based, most of the genes recovered were cilia-related, including genes encoding proteins important for ciliogenesis, cilia-transduced cell signaling, and vesicular trafficking. Also unexpected, many of the cilia related genes recovered are known direct protein-protein interactors, even though each gene was recovered independently in unrelated mouse lines. These findings suggest a cilia-based protein-protein interactome network may provide the context for congenital heart disease pathogenesis. This could explain the incomplete penetrance and variable expressivity of human CHD, and account for its complex non-Mendelian etiology. Supporting these findings in mice, a preponderance of cilia and cilia related cell signaling genes were observed among de novo pathogenic variants identified in a CHD patient cohort. Further clinical relevance unfolded with the observation of a high prevalence of respiratory cilia dysfunction in CHD patients. This was associated with increased postsurgical respiratory complications. Together these findings highlight the importance of cilia in CHD pathogenesis and suggest possible clinical translation with instituting pulmonary therapy to improve outcome for CHD patients undergoing congenital cardiac surgeries.

1. Introduction: the genetic etiology of CHD

Congenital heart disease (CHD) is one of the most prevalent birth defects, affecting up to 1% of live births [1,2]. Despite strong evidence for its genetic underpinning, the genetic landscape of CHD is still not well understood. CHD is observed to be sporadic and associated with autosomal dominant inheritance with two to three-fold more affected males then females [3]. Genetic analysis has been hampered by the inherent genetic heterogeneity of the human population. Further complicating matters is the incomplete penetrance and variable expressivity associated with CHD [4–6]. Thus, some individuals with known pathogenic mutation may have no disease, while others may have CHD but of differing phenotype. These challenges have made progress slow, although with large cohorts of CHD patients being sequenced, insights are emerging that promise more rapid progress in the near future [7–9].

2. Modeling congenital heart defects in mice

Given challenges faced by genetic studies in the human population, modeling CHD in mice offers a valuable alternative. Inbred mouse strains are readily available, and their genomes have been completely sequenced, well annotated, and are nearly identical to that of human [10,11]. Most importantly, mice have the same cardiovascular anatomy that are the substrates of CHD, including a four-chamber heart with two outflows mediating separate pulmonary vs. aortic circulation that provides efficient oxygenation of blood [12]. Studies of many knockout and mutant mouse models have shown the feasibility to model a wide spectrum of CHD in mice [13]. Hence inbred mice provide a valuable model system to study the genetic and developmental etiology of CHD.

3. Large scale mouse forward genetics

Forward genetics provides a valuable complement to the use of reverse genetics to interrogate the genetic etiology of CHD. While reverse genetics provide access to knockout and knockin mutations in selected genes of interest, with forward genetics mutations are randomly introduced into the genome, and genes causing CHD can be recovered using a phenotype-based screen to identify mutants with structural heart defects. This approach, being non-gene biased, comprises a “systems genetics” approach that can yield not only novel genes but by examining the totality of genes, identify novel pathways that may give new insights into the pathogenic mechanisms driving CHD.

There are multiple experimental approaches available to conduct forward genetic screens in mice. One method developed entailed the use of gene trap constructs in embryonic stem cells to disrupt gene function [14]. With this approach, the gene trap vector is inserted randomly in the genome of mouse embryonic stem cells (ES) to generate ES cells with random mutations distributed throughout the genome. Such a library of ES cells can then be screened by PCR and

* Corresponding author.
E-mail address: cel36@pitt.edu (C.W. Lo).

https://doi.org/10.1016/j.ppedcard.2019.101128
Received 11 June 2019; Accepted 8 July 2019
Available online 10 July 2019
1058-9813/

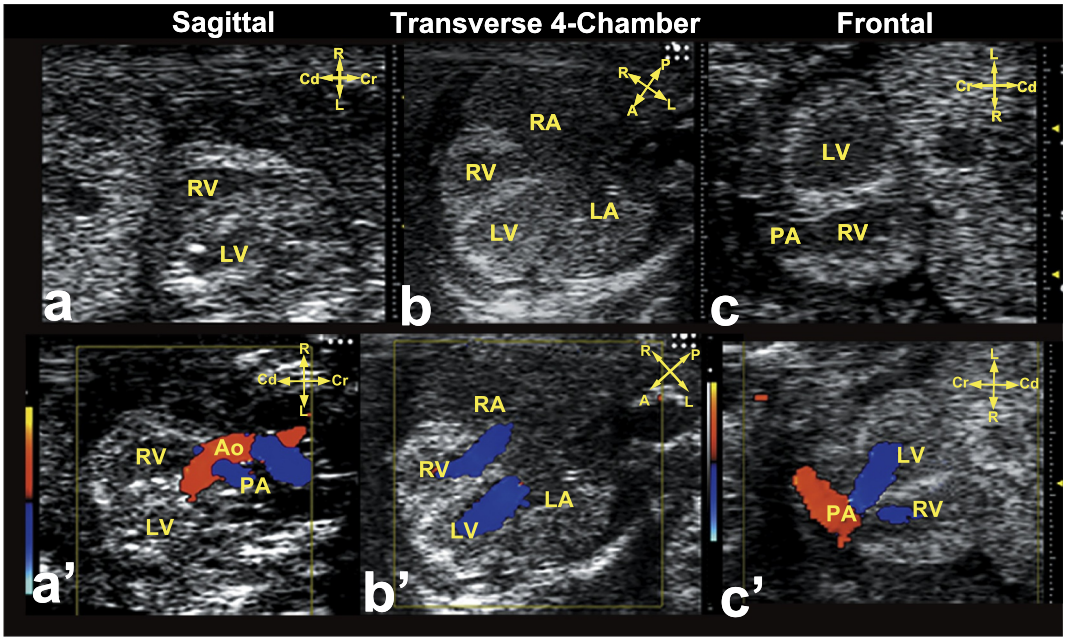

Fig. 1. Ultrasound imaging planes for cardiovascular phenotyping in fetal mice.
Cardiac diagnosis with ultrasound biomicroscopy is performed using sagittal (a and a'), transverse 4-chamber (b and b′), and frontal (c and c′) imaging planes. Note that the anterior–posterior axis is equivalent to the body's dorsal–ventral axis. A indicates anterior; Cd, caudal; Cr, cranial; L, left; P, posterior; and R, right. Adapted from Liu et al. Circ Cardiovasc Imaging 2014 [23].

sequencing analysis to recover ES clones with mutations in genes of interest. The main advantage of this approach is the ease with which the mutation can be quickly identified through the gene trap vector. However, these mutations are largely loss of function mutations, and often can involve alternative splicing triggered by the gene trap insertions that may complicate the downstream analysis. Yet another method for forward genetics entails the insertion of transposons such as Sleeping beauty or piggy bac transposons that are activated in the germline [15,16]. As this approach entails direct mutagenesis in the oocyte, it provides direct access to the production of mice harboring random mutations. However, the integration of these transposons is not random, and this technique is best suited for generating a cluster of mutations in different loci in the mouse genome.

The current method of choice and the most commonly used platform for forward genetics in mice is that of chemical mutagenesis using the mutagen ethylnitrosourea (ENU) [17]. ENU mutagenesis generates point mutations that can yield missense mutations, or null mutations comprising stop-gain or splicing mutations. Hence, ENU mutagenesis provides access to missense mutations not accessible with either gene trap or transposon mediated mutagenesis. The main disadvantage of ENU mutagenesis is the previous difficulty in mutation recovery. Prior to the availability of whole exome or whole genome sequencing analysis, mutation recovery involved very time consuming and cumbersome mapping of the mutation followed by positional cloning for mutation recovery. This bottleneck was a stumbling block that led many labs and funding agencies to abandon pursuing this powerful tool for large scale forward genetics. With inexpensive next generation sequencing the mutation recovery bottleneck has been resolved, and now the key to the successes of forward genetic screens rides on the robustness of the phenotyping protocol. Thus, some striking successes have emerged in recent years from disparate large-scale screens, such as those conducted to delineate genes regulating circadian rhythm, immune disorder, or by our laboratory, genes and pathways associated with CHD [18–21].

4. Cardiovascular phenotyping with fetal echocardiography

To pursue our large scale ENU mutagenesis screen for mutations causing CHD, we developed the use of noninvasive fetal echocardiography for cardiovascular phenotyping in mice [22]. Echocardiography is ideally suited for cardiovascular phenotyping given it is a noninvasive clinical imaging modality developed specifically for cardiac exam, including the diagnosis of CHD. Because it is noninvasive, it allows for high throughput phenotyping and tracking of disease progression with longitudinal interrogation of the same fetuses over a period of days. However, given the very small size of fetal mouse heart (only 3.0 mm near term) as compared to that of human fetuses, the diagnosis of CHD in fetal mouse cannot be accomplished using clinical ultrasound systems. Instead we use the Vevo2100 ultra-high frequency ultrasound biomicroscope equipped with a 40 MHz transducer that can achieve 10× higher spatial resolution than traditional clinical ultrasound systems [23].

Ultrasound scanning was conducted from E15.5 to near term at E18.5. When there was evidence of embryonic lethality, earlier ultrasound scans were pursued at E13.5–15.5. This developmental window was selected for screening as we previously showed two peaks of prenatal death in ENU mutagenized mice, the first occurring at E12.5 and the second at E15.5–16.5 [24]. Given our interest was to recover mutations relevant to human CHD, we chose to focus our screen around the later time of death when outflow septation and formation of the 4-chamber heart is complete. This would then allow the emergence of defect phenotypes relevant to CHD observed clinically. The ultrasound scans were conducted using three imaging planes adapted from those used clinically using as a reference the body axis of the fetus, i.e. sagittal, transverse 4-chamber, and frontal views. This is necessary since each pregnant dam typically will have 6 to 8 fetuses. With the sagittal imaging plane, it is possible to examine the relative placement of the aortic and pulmonary arteries (Fig. 1a,a'). In the transverse 4-chamber view, the atrioventricular connections can be examined (Fig. 1b,b'), while in the frontal view, the ventriculoarterial connections can be examined (Fig. 1c,c').

Most of the structural heart defects observed clinically were also

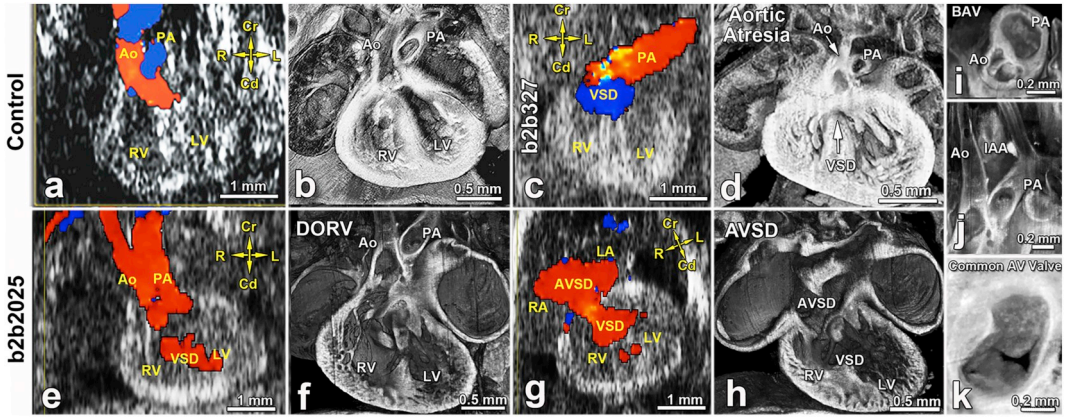

Fig. 2. Ultrasound diagnosis of congenital heart disease.
a, b, Color flow imaging of a wildtype mouse embryo shows normal aorta (Ao) and pulmonary artery (PA) alignment (a) confirmed by histopathology (b). c, d, Embryonic day (E)16.5 mutant mouse (line b2b327) exhibited a blood flow pattern indicating single great artery (pulmonary artery) and ventricular septal defect (VSD) (c), suggesting aortic atresia with ventricular septal defect, confirmed by histopathology (d). e–h, Color flow imaging of E15.5 mutant mouse (line b2b2025) with heterotaxy (stomach on right) showed side by side aorta and pulmonary artery, with the aorta emerging from the right ventricle, indicating DORV/ventricular septal defect (e, f) and the presence of AVSD (g, h). i–k, Histopathology also showed a bicuspid aortic valve (BAV) (i), interrupted aortic arch (IAA) (j), and common atrioventricular (AV) valve (k). Cd, caudal; Cr, cranial; L, left; LV, left ventricle; R, right; RV, right ventricle; LA, left atrium; RA, right atrium. (For interpretation of the references to color in this figure legend, the reader is referred to the web version of this article.)
Adapted from Li et al. Nature 2015 [21].

Table 1
Efficiency of cardiovascular phenotyping with Acuson vs. Vevo2100.
Adapted from Liu et al. Circ Cardiovasc Imaging 2014 [23].

Ultrasound diagnosis	Acuson[a]	Vevo2100[a]	P-value[†]
Abnormal echocardiography findings n = (1457)			
Cardiac structural defects (n = 352; 24%)			
Septal defects	**17 (4.8%)**	**241 (68.5%)**	**< 0.01**
VSD	15 (4.3%)	176 (50%)	< 0.01
AVSD	2 (0.6%)	65 (18.5%)	< 0.01
Outflow tract defects	**12 (3.4%)**	**127 (36.1%)**	**< 0.01**
DORV/overriding aorta	9 (2.6%)	75 (21.3%)	< 0.01
With VSD	9 (2.6%)	57 (16.2%)	< 0.01
With AVSD	0 (0%)	18 (5.1%)	< 0.01
With pulmonary stenosis	0 (0%)	17 (4.8%)	< 0.01
PTA/PA	3 (0.9%)	38 (10.8%)	< 0.01
With VSD	3 (0.9%)	25 (7.1%)	< 0.01
With AVSD	0 (0%)	13 (3.7%)	< 0.01
TGA	**0** (0%)	14 (4.0%)	< 0.01
With VSD	0 (0%)	13 (3.7%)	< 0.01
With AVSD	0 (0%)	1 (0.3%)	1.000
With pulmonary stenosis	0 (0%)	1 (0.3%)	1.000
Left heart obstruction lesions	**7 (2.0%)**	**23 (6.5%)**	**< 0.01**
Mitral atresia/stenosis	0 (0%)	8 (2.3%)	< 0.05
Aortic atresia/stenosis/coarctation	7 (2.0%)	15 (4.3%)	0.087
Hypoplastic left heart syndrome	0 (0%)	4 (1.1%)	0.133
Right heart obstruction lesions	**10 (2.8%)**	**50 (12.2%)**	**< 0.01**
Tricuspid atresia/hypoplasia	0 (0%)	15 (4.3%)	< 0.01
Pulmonary stenosis	10 (2.8%)	35 (9.9%)	< 0.01
Hypoplastic right heart syndrome	0 (0%)	11 (3.1%)	< 0.01
Coronary artery fistula	**4 (1.1%)**	**8 (2.3%)**	**0.247**
Cardiac situs anomalies	**0** (0%)	**40 (11.4%)**	**< 0.01**
Dextrocardia	0 (0%)	34 (9.7%)	< 0.01
Mesocardia	0 (0%)	6 (1.7%)	< 0.05
Non-specific abnormal findings (n = 1105)			
Total arrhythmia	**262**	**262**	**1.000**
Without structural defects	103	103	1.000
Total hydrops/pericardial effusion	**598**	**635**	**0.165**
Without structural defects	324	364	0.08
Total hemodynamic perturbations[b]	**1030**	**1100**	**0.190**
Mild without structural defects	670	678	0.766

[a] Values in parentheses represent percentage of affected fetuses among 352 fetuses scanned by Acuson and UBM and identified with CHD.
[b] Hemodynamic perturbations including inflow and OFT increased velocity and regurgitation.
[†] P-values based Chi-square analysis.

found in our CHD mouse mutants, such as aortic atresia (Fig. 2c,d), double outlet right ventricle (DORV) (Fig. 2e,f), and atrioventricular septal defects (AVSD) (Fig. 2g,h) (Table 1). In contrast, ultrasound scans conducted with the Acuson Sequoia clinical system, even using a 15 MHz vascular transducer missed most septal defects and outflow tract anomalies, as well as other complex structural heart defects (Table 1) [23]. However, the detection of arrhythmias, pericardial effusion/hydrops and other hemodynamic perturbations are detected equally by both ultrasound systems (Table 1). Follow up confirmation analysis with necropsy and 3D histological reconstructions using episcopic confocal microscopy showed ultrasound scans conducted with the Visualsonics ultrasound system provided > 95% accuracy in the diagnosis of most CHD, including coronary fistulas, pulmonary stenosis, coarctation and aortic stenosis, and mitral valve atresia/stenosis (Table 2) [23]. Even complex CHD such as transposition of the great arteries or HLHS could be accurately diagnosed using the ultra-high frequency ultrasound system (Fig. 3, Tables 1,2).

5. Prevalence of different structural heart defect phenotypes

A wide spectrum of CHD phenotypes was observed in our mouse mutagenesis screen, the most prevalent being ventricular septal defects (VSD), seen in 68.5% of the fetuses identified with CHD (Table 1). VSD is also the most common CHD seen in the human population [1]. In comparison, the rarest CHD detected was HLHS, seen in 1.1% of the fetuses identified with CHD (Fig. 3) [25]. Clinically, HLHS is also relatively rare in the human population, seen in 2–3% of CHD cases [26,27]. We note prior to the recovery of HLHS mutants in our screen, HLHS had never been seen in mice before. This likely is explained by our subsequent studies that indicated HLHS has a requisite multigenic etiology [25].

OFT anomalies were relatively common, found in 36% of the CHD mutants. Among these, the most prevalent was DORV/overriding aorta (21%), followed by persistent truncus arteriosus (PTA) (10.8%), then transposition of the great arteries (TGA, 4%; Table 1) [21]. OFT anomalies were often observed to be accompanied by muscular VSDs or AVSD (Table 1). It should be noted 23% of the mutants with DORV/overriding aorta also had pulmonary stenosis (Table 1). Given these phenotypes are presenting in fetal mice, they may have relevance to the emergence of Tetralogy of Fallot postnatally. Thus, RV hypertrophy could be elicited postnatally by hemodynamic remodeling occurring

Table 2
Accuracy of fetal echocardiography diagnosis of congenital heart disease.
Adapted from Liu et al. Circ Cardiovasc Imaging 2014 [23].

CHD diagnosis	CHD confirmed[c]	CHD missed[d]	Sensitivity[e]	Specificity[f]	Accuracy[g]
Septal defects[a]	156/163	67/275	70% (156/223)	96.7% (208/215)	83.1%
Outflow tract defects[b]	105/123	25/315	80.8% (105/130)	94.2% (290/308)	90.2%
HLHS	4/4	0/434	100% (4/4)	100% (434/434)	100%
HRHS	7/9	2/429	77.8% (7/9)	99.5% (427/429)	99.1%
MS/MA	6/8	2/430	75% (6/8)	99.5% (428/430)	99.1%
AS/AA/COA	9/15	20/423	31% (9/29)	98.5% (403/409)	94.1%
Tricuspid hypoplasia/atresia	6/10	4/429	60% (6/10)	99.1% (425/429)	98.4%
Pulmonary stenosis	9/10	15/428	37.5% (9/24)	99.8% (413/414)	96.3%
Coronary artery fistula	5/7	9/431	35.7% (5/14)	99.5% (422/424)	97.5%
Cardiac situs defects	18/18	4/420	81.8% (18/22)	100% (416/416)	99.1%

HLHS = hypoplastic left heart syndrome; HRHS = hypoplastic right heart syndrome; MS/MA = mitral valve stenosis/mitral valve atresia; AS/AA/COA = aortic stenosis/aortic atresia/coarctation.

[a] Ventricular septal defects, atrioventricular septal defects.
[b] Transposition of the great arteries, double outlet right ventricle, persistent truncus arteriosus.
[c] CHD Diagnoses Confirmed = (no. of confirmed fetal echocardiography CHD diagnoses) / (total no. of fetal echocardiography CHD diagnoses).
[d] Missed CHD Diagnosis = (no. of confirmed false-negative "No-CHD" fetal echocardiography diagnoses) / (total no. fetal echocardiography "No-CHD" diagnoses).
[e] Sensitivity = (no. of confirmed fetal echocardiography "CHD" diagnoses) / (no. of confirmed CHD + no. of confirmed false-negative "No-CHD" diagnoses).
[f] Specificity = (no. of confirmed "No-CHD" diagnoses) / (no. of confirmed "No-CHD" diagnoses + no. of confirmed false-positive "CHD" diagnoses).
[g] Accuracy = (no. of confirmed "CHD" + no. of confirmed "No-CHD" diagnoses) / (total no. of fetal echocardiography scanned fetuses.

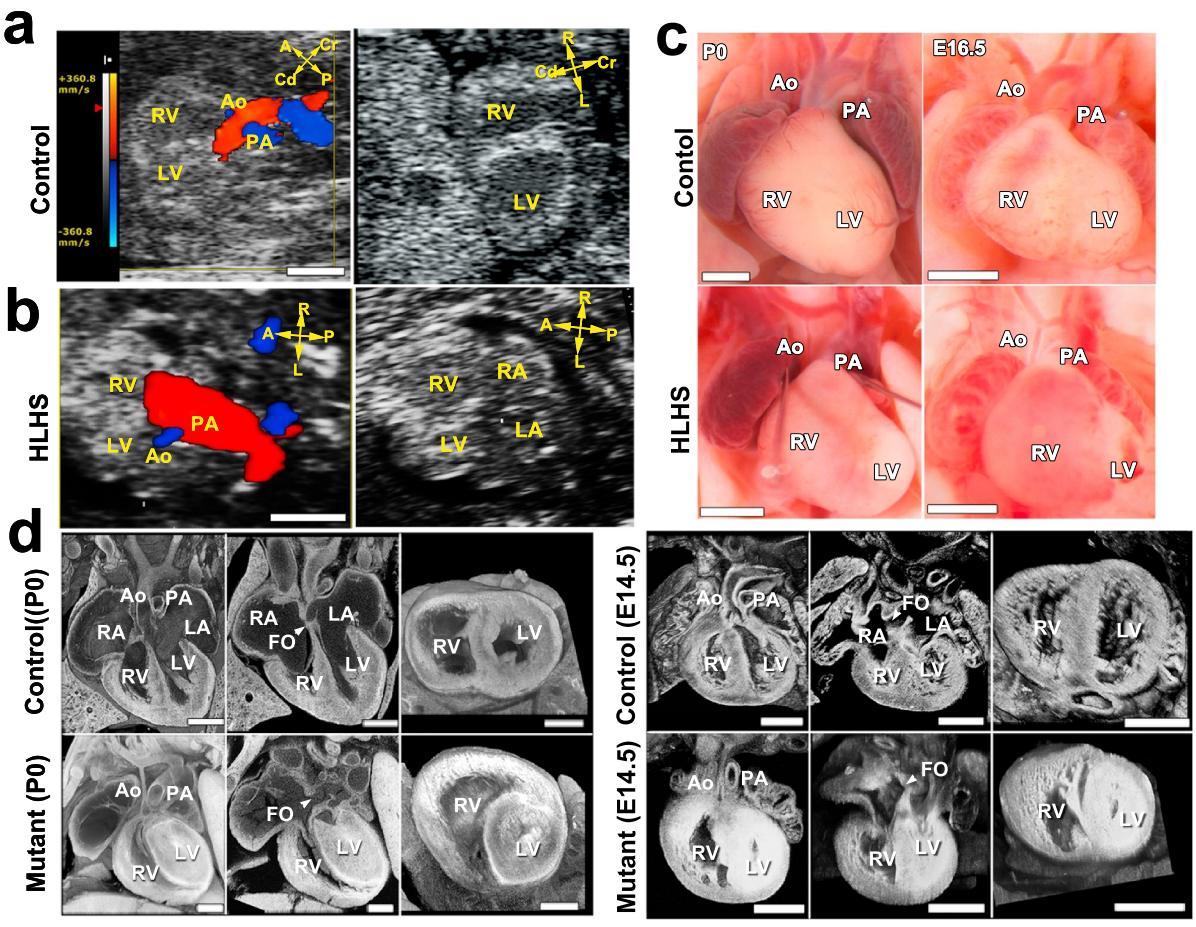

Fig. 3. First mouse model of hypoplastic left heart syndrome recovered from ENU mutagenesis screen.
(a–d) HLHS mutant mice display cardinal features of HLHS. (a,b) Ultrasound color-flow imaging of normal fetus (a), showing robust flow from the aorta (Ao) and pulmonary artery (PA). In the HLHS mutant (b), the aorta showed only a narrow flow stream, whereas the pulmonary artery showed robust flow. 2D imaging revealed hypoplastic LV (b), as compared with the normal-sized LV in the control (a). (c) Newborn (P0) or E16.5 hearts from wild-type and HLHS mutants. Hypoplastic aorta and LV are visible in the HLHS mutant. (d) Histopathology showing the cardiac anatomy of HLHS mutant and littermate control at birth (P0) and E14.5. Compared with controls, the HLHS mutant exhibited hypoplastic aorta and aortic valve atresia, hypertrophied LV with no lumen, MV stenosis and patent foramen ovale (FO), arrowhead. LA, left atrium; RA, right atrium; A, anterior; P, posterior; L, left; R, right; Cr, cranial; Cd, caudal. Scale bars: a,b, 0.5 mm; c, 1 mm; d, 0.5 mm. (For interpretation of the references to color in this figure legend, the reader is referred to the web version of this article.)
Adapted from Liu et al. Nature Genetics 2017 [25].

due to restricted blood flow from the pulmonary trunk.

Cardiac situs defects were observed at surprisingly high incidence (Table 1) [21]. The cardiovascular system is the most left-right asymmetric organ system in the body and this asymmetry generates the pulmonary vs. systemic circulation needed for efficient oxygenation of blood. Some of the most complex CHD were seen in mutants with cardiac and/or visceral organ laterality defects, similar to the well described clinical association of complex CHD with heterotaxy. Our heterotaxy mutants typically died prenatally, which is consistent with the previous finding of > 50% prenatal/intrauterine deaths in human fetuses with heterotaxy [28–30]. We note in one study, 16% of human fetuses with CHD were found to have heterotaxy [31]. These findings, together with a report indicating only 28% of CHD is prenatally diagnosed, would suggest a large fraction of human conceptuses with heterotaxy and CHD are not accounted for in the clinical CHD population [32]. Hence CHD associated with heterotaxy is likely much more prevalent than realized, overall consistent with the findings from our mouse screen.

6. Cilia mutations in the pathogenesis of CHD

Our screen used a classic two generation G2XG1 backcross breeding scheme to screen for recessive mutations causing CHD in the G3 fetuses [21]. G1 males were mated with C57BL6 wildtype mice to generate G2 daughters and these were mated back to the G1 males to generate G3 offspring. G2 pregnant dams were ultrasound scanned to interrogate for cardiovascular defects in the G3 fetuses. The high throughput nature of noninvasive ultrasound imaging made it possible to screen over 100,000 G3 fetal mice from 3000 G1 pedigrees [21]. This yielded over 300 mutant lines with a wide spectrum of CHD phenotypes, including the first mouse models of HLHS as described above [25]. Given the screen was conducted in C57BL6 inbred mice, mutation recovery was straight forward and entailed the use of whole exome sequencing (WES) analysis. This was typically carried out in just one mutant from each line, followed by genotyping analysis to identify the one mutation that is consistently homozygous across all the mutants with the same CHD phenotype.

As expected for ENU mutagenesis, most of the mutations recovered were missense, with the remainder equally divided between splicing defect vs. stop gain mutations (Fig. 4A,B,C). At the midpoint of our screen, 91 pathogenic mutations were recovered in 61 genes (Fig. 4D) [21]. Among the pathogenic mutations, 19 were splicing mutations, with 5 more than 2 bases away from the canonical splice donor/acceptor sites. Multiple pathogenic mutations were recovered in 15 genes, indicating the screen was moving towards saturation. Surprisingly, 35 of the 61 genes recovered with CHD causing mutations were cilia related (Fig. 4C). This included both motile (34%) and primary (66%) cilia related genes. As the screen was phenotype based and agnostic towards any specific genes or pathway, this enrichment for cilia genes was unexpected. This included many genes encoding proteins in the cilia transition zone that regulates gating of cilia protein trafficking, as well components of the basal body and centrosome, the intraflagellar transport (IFT) system, and also components required for motile cilia assembly/function (Fig. 5).

7. Three situs outcomes with CHD only with heterotaxy

Many of the cilia related genes caused CHD in conjunction with laterality defects. This included both primary and motile cilia related genes, a reflection of the known importance of motile and primary cilia in the regulation of left-right patterning [33]. However, it should be noted that the importance of cilia in CHD pathogenesis goes beyond the regulation of left-right patterning, as many of the primary cilia related genes (34%) causing CHD do not disturb left-right patterning [21]. Among cilia genes causing CHD associated with laterality disturbance, 13 are genes required for motile cilia function and are known to cause primary ciliary dyskinesia (PCD), a sinopulmonary disease associated with mucociliary clearance deficits due to dyskinetic or immotile cilia in the airway. This included mutations in genes encoding outer dynein arm components (*Dnah5*, *Dnah11*, etc.) required for motor activity, cilia basal body proteins (such as *Mks1*, *Cep110*), cilia transition zone components (*Cc2d2a*, *Nek8,* etc.), as well as cytoplasmic motile cilia assembly factors (*Dyx1c1*, *Armc4*, etc.) (Fig. 5).

PCD patients have long been known to have a high prevalence of situs inversus with mirror symmetric visceral organ situs, also known as Kartagener's syndrome [34]. These longstanding observations suggested a mechanistic link between PCD and left-right patterning which we now appreciate as reflecting the essential role of motile cilia in embryonic left-right patterning. The association of PCD with heterotaxy and CHD was not well recognized until studies in mice showed mutations in *Dnah5*, a gene known to cause PCD, can yield mutants with heterotaxy and CHD [35]. Findings from the *Dnah5* mutants revealed the same *Dnah5* mutation can yield offspring with three distinct laterality phenotypes, including situs solitus with normal visceral organ situs, situs inversus with mirror symmetric visceral organ situs, as well as heterotaxy (Fig. 6) [35,36]. Importantly, CHD was seen only in the *Dnah5* mutants with heterotaxy [35].

The association of CHD with heterotaxy was in fact observed for all 13 PCD genes recovered from our screen. They all yielded an identical presentation with mutants exhibiting three situs phenotypic outcomes, but with CHD seen only in mutants with heterotaxy. Typically, 50% of the homozygous mutants will have heterotaxy and CHD, while the other 50% will exhibit situs solitus or situs inversus without CHD. Clinical analysis of PCD patients for laterality defects and CHD have indicated a lower penetrance of CHD and heterotaxy. Thus, one study showed 6.3% of PCD patients have CHD, while another study showed heterotaxy is present in 12% of PCD patients [37,38]. We expect this much lower incidence of heterotaxy and CHD in the PCD population may reflect ascertainment bias. As discussed above, a high incidence of prenatal demise has been observed among human fetuses with complex CHD associated with heterotaxy. Consistent with this, we also noted mice with heterotaxy and complex CHD often died in utero.

It is important to note that the finding of three situs phenotypes associated with mutations causing CHD associated with heterotaxy is not limited to mutations in genes required for motile cilia function. This is also observed for mutations causing CHD associated with primary cilia related genes. As with the motile cilia mutations, mutations in these genes cause CHD only with heterotaxy, while mutants with situs solitus or situs inversus phenotypes have no cardiovascular defects. These findings suggest human genetic analysis for genes causing CHD associated with heterotaxy can be confounded by individuals in the population bearing pathogenic mutations but not presenting with any disease phenotypes. These findings suggest a different paradigm is required for interrogating the genetic etiology of mutations causing CHD associated with heterotaxy.

8. Ciliopathy genes causing CHD

Some of the CHD causing mutations in primary cilia related genes are associated with human diseases referred to collectively as ciliopathies [39]. This included many proteins found in the cilia transition zone and basal body. For example, CHD causing mutations were recovered in *Anks6* and *Nek8*, encoding transition zone proteins known to cause nephronophthisis, a ciliopathy associated with cystic renal disease [40]. Anks6 is an ankyrin repeat protein that is a known protein-protein interactor of Nek8 and is the only known substrate of the Nek8 kinase [40]. A CHD causing mutation was recovered in *Jbts17*, a gene encoding a cilia transition zone protein that is the gene most commonly responsible for Joubert syndrome, a cerebellar dysplasia characterized by the imaging marker known as the molar tooth sign [41,42]. Also associated with Joubert syndrome is *Cc2d2a*, a gene encoding another cilia transition zone protein recovered in our screen [43]. We also

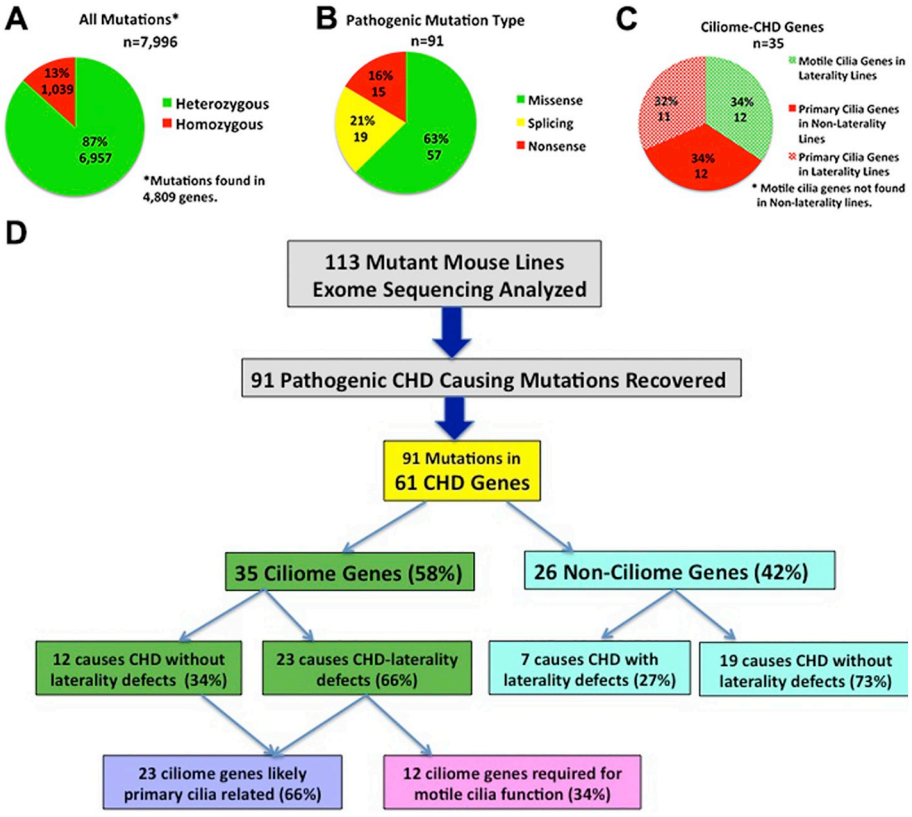

Fig. 4. Distribution of pathogenic mutations and ciliome mutations causing CHD recovered from ENU mutagenesis screen.
a, Distribution of all incidental coding mutations (left), pathogenic mutations (middle) and ciliome CHD genes (right) recovered from 113 CHD mouse mutant lines. b, A flow chart showing the distribution of ciliome versus non-ciliome CHD genes among laterality versus non-laterality CHD lines, and further stratification of ciliome CHD genes affecting primary versus motile cilia function.
Adapted from Li et al. Nature 2015 [21].

recovered a mutation in *Mks1*, a gene associated with Meckel syndrome (MKS) [44]. This ciliopathy involves severe birth defects associated with multiorgan system anomalies [45]. Due to the severe developmental phenotypes associated with MKS, fetuses with MKS are usually aborted or stillborn [46]. Additionally, we recovered mutations in *Cep290* which encodes another transition zone protein associated with many different ciliopathies and thus may act as a modifier in different ciliopathies [47]. The recovery of CHD causing mutations in these various ciliopathy genes was somewhat surprising, since structural heart defects are not a common finding in ciliopathies, although it is not unheard of either. In this regard, it is important to note that we have found most of these ciliopathy genes are in fact essential for normal left-right patterning. They typically cause laterality defects with the three phenotypic outcomes as described above, with CHD seen only with

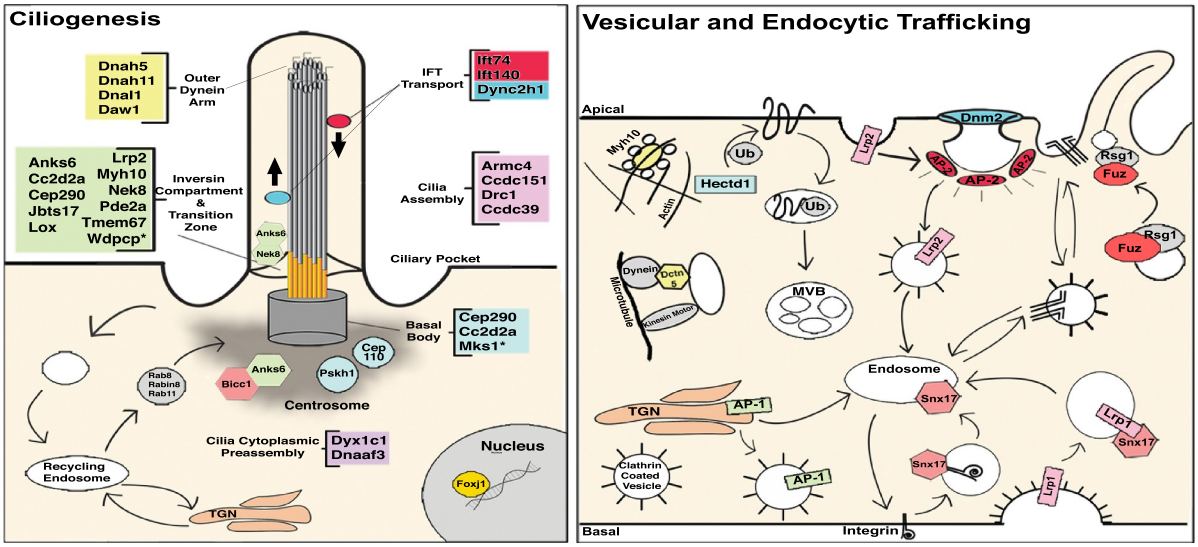

Fig. 5. CHD genes recovered from ENU mutagenesis screen.
These diagrams illustrate biological context of CHD gene function in ciliogenesis or vesicular and endocytic trafficking. Color highlighting indicates a CHD gene recovered in the ENU mutagenesis screen. For clarity, ciliome genes (*Dctn5*, *Fuz*) with endocytic function and/or involved in cilia-transduced signaling are not shown in the ciliogenesis panel. AP, adaptor protein complex; R, receptor; MVB, multi-vesicular body; TGN, *trans*-Golgi network; Ub, ubiquitination. (For interpretation of the references to color in this figure legend, the reader is referred to the web version of this article.)
Adapted from Li et al. Nature 2015 [21].

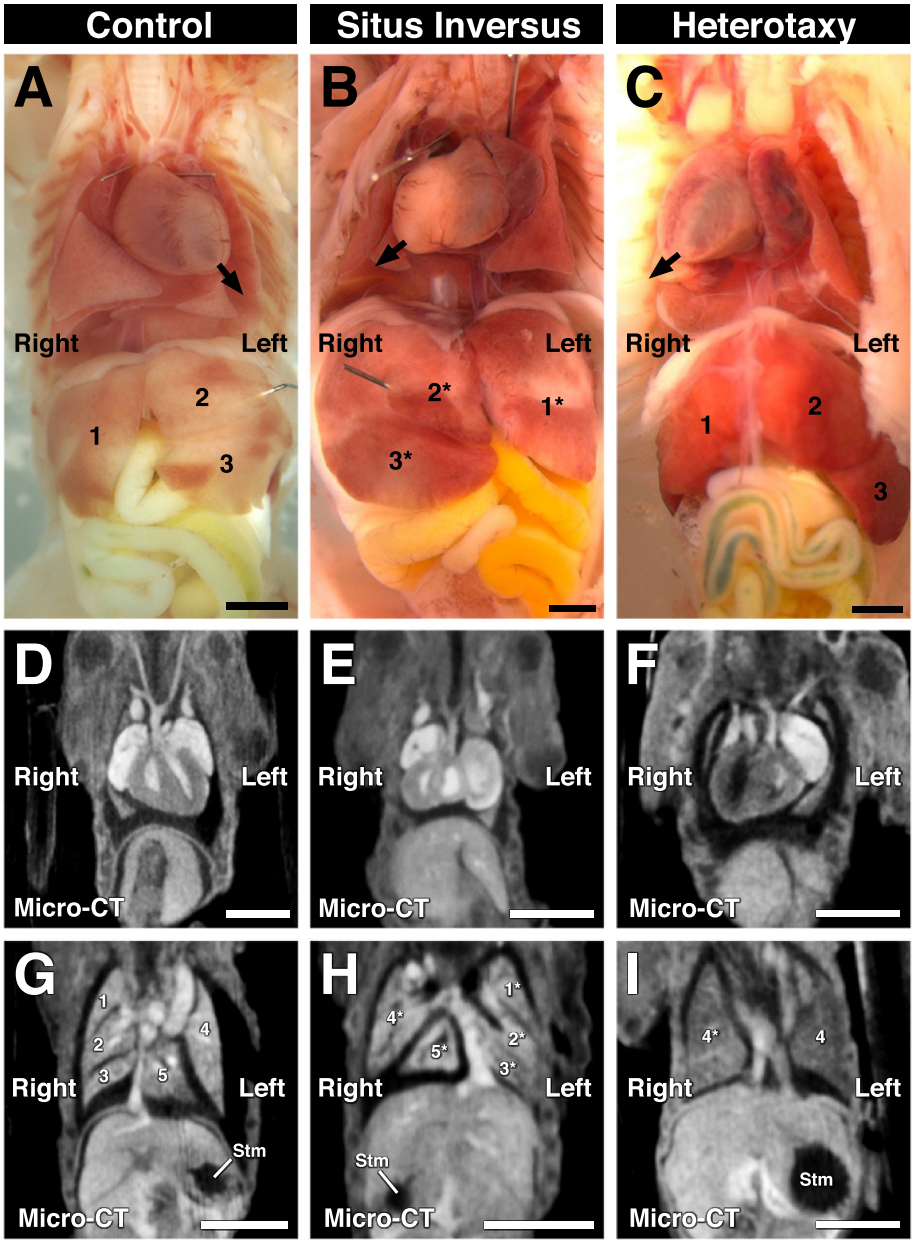

Fig. 6. *Dnah5* mutations result in three distinct laterality phenotypes.
Necropsy (A–C) and corresponding micro-CT (D–I) images of newborn mice with normal placement of visceral organs (A, D, G), situs inversus totalis with complete mirror reversal of organ situs (B, E, H), and heterotaxy with left–right randomized organ situs (C, F, I). The mutant pup exhibiting situs inversus possesses a right-sided heart (dextrocardia), left-sided inferior vena cava, inversion of lung and liver lobes, and a right-sided stomach (A, D, G), whereas the mutant pup exhibiting heterotaxy showed dextrocardia, duplicated inferior vena cava left-pulmonary isomerism, normal liver lobation, and a left-sided stomach (C, F, I). Arrows denote the direction to which the heart apex is pointing; asterisks indicate mirrored organ positioning. Scale bar = 2.5 mm. Stm, stomach.
Adapted from Kim et al. Circ Cardiovasc Imaging 2013 [36].

heterotaxy. Hence, CHD may be under appreciated in these ciliopathies if the heterotaxy/CHD fetuses are largely inviable to term. It is interesting to note that mutation in *Jbts17* causing Joubert syndrome is one of the few ciliopathy genes we recovered that did not cause laterality defects. Notable is the fact that the *Jbts17* mutants exhibited a spectrum of phenotype severity in the cardiovascular system, ranging from mutants with normal heart structure to those with CHD comprising pulmonary stenosis to pulmonary atresia [41]. In contrast to the variability in the cardiac phenotype, birth defects involving other structures including the cerebellar dysplasia were seen more consistently across all mutants. Together these findings suggest ciliopathies may have a broader role to play in CHD pathogenesis than previously appreciated.

9. Role of cilia transduced cell signaling in CHD pathogenesis

The enrichment of cilia related genes points to cilia biology playing an important role in developmental processes underlying the pathogenesis of CHD. This likely involves cilia transduced SHH, TGFβ, PDGF, and Wnt/PCP signaling. These cell signaling pathways are known to play important roles in many different developmental processes regulating cardiac morphogenesis, such as SHH regulation of the deployment of the second heart field that will form the outflow tract, or the role of PDGF in regulating delamination of cardiac neural crest cells required for outflow tract septation [48,49]. TGFB and Wnt signaling play important roles in endocardial epithelial-mesenchymal transformation required for cardiac cushion formation and valvular morphogenesis [50]. Indeed, examination of a *Cc2d2a* mutant exhibiting atrioventricular (AV) septal defect showed specific loss of cilia in the AV cushions, but not in the unaffected outflow cushions (Fig. 7).

Supporting the importance of these cilia transduced cell signaling pathways in CHD, we also recovered 16 CHD causing mutations in genes that mediate cilia transduced cell signaling, such as those involved in SHH, TGFβ, PDGF, and Wnt/PCP signaling [21]. In addition, we also recovered 10 mutations in genes involved in endocytic/vesicular trafficking (Fig. 5). This is not a pathway previously known to play a role in CHD, but vesicular trafficking is essential in the regulation of ciliogenesis and cilia transduced cell signaling [51]. Hence, in totality, the large majority of CHD genes (53 of 61) recovered from our

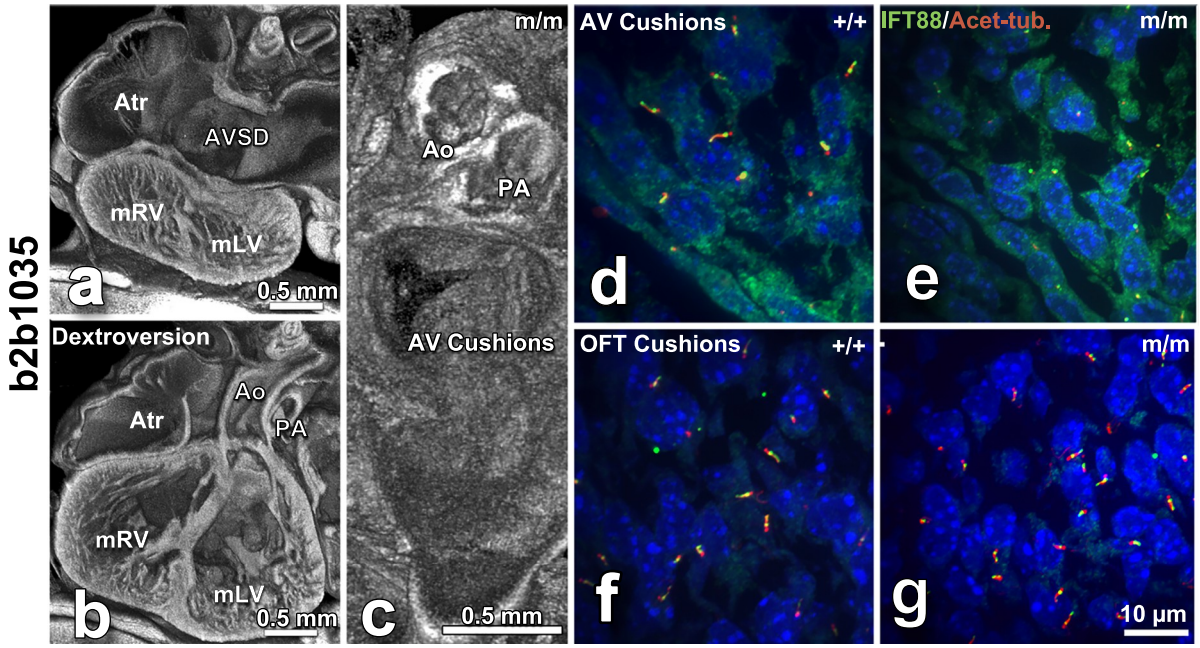

Fig. 7. *Cc2d2a* mutant mice show laterality defects, impaired atrioventricular cushion development, and cilia defects.
a–c, *Cc2d2a*-mutant mouse exhibits dextrocardia with ventricular inversion (dextroversion) (b), and AVSD (a) with malformed atrioventricular cushions (c), but normal outflow cushions. d-g, Confocal imaging of E12.5 *Cc2d2a*-mutant mouse (m/m) versus wild-type (+/+) embryo sections showed no cilia in the atrioventricular cushion (d,e), but normal ciliation in the outflow cushion (OFT cushion) (q,f,g). Red, acetylated tubulin (Acet-tub.); green, IFT88. Atr, atrium; mLV, morphologic left ventricle; mRV, morphologic right ventricle; Ao, aorta; PA, pulmonary artery; AVSD, atrioventricular septal defect. (For interpretation of the references to color in this figure legend, the reader is referred to the web version of this article.)
Adapted from Li et al. Nature 2015 [21].

forward genetic screen are cilia related - whether comprising cilia genes, cilia transduced cell signaling genes, or genes involved in endocytic/vesicular trafficking. We note cilia also may have important roles in the regulation of cell proliferation and apoptosis, and hence may contribute to CHD pathogenesis through the regulation of progenitor pools or tissue remodeling mediated by apoptosis [52]. Further studies into the pathogenic mechanism by which cilia drives CHD pathogenesis may provide insights to guide clinical care and improve patient outcome.

10. Role for cilia in human CHD

The central role of cilia in CHD revealed by the mouse forward genetic screen raises the question of the role of cilia in human CHD. To address this question, we leveraged the previous whole exome sequencing data of CHD patients generated by the Pediatric Cardiac Genomics Consortium [53]. Whole exome sequencing analysis was conducted on trios and 28 de novo predicted pathogenic mutations were identified [53]. Of these, 3 are in cilia genes, 7 in cilia transduced TGFβ/SHH/Wnt signaling and 2 are involved in vesicular/endocytic trafficking (Table 3). Furthermore, a mutation was also recovered in *PITX2*, a gene essential for left–right patterning. As this was recovered in a non-heterotaxy patient, this suggested a broader role for left–right patterning in CHD pathogenesis. Together these 13 genes comprise nearly half of all the de novo pathogenic mutations recovered from the CHD patients, confirming cilia and cilia related pathways identified in the mouse forward genetic screen have significant relevance to the genetic etiology of human CHD.

11. Case for complex genetics

Another notable finding from the mouse forward genetic screen was that many of the genes recovered encoded proteins that are direct protein-protein interactors (PPI), such as Anks6 and Nek8 mentioned above. In addition, a CHD causing mutation was recovered in *Bicc1*, which is a direct binding partner of *Anks6*, and also in *Wwtr1*, which is a known binding partner of *Nek8* [54,55]. Previous proteomic analysis by mass spectrometry identified three PPI modules that correlated with the ciliopathies nephronophthisis (NPHP), Joubert Syndrome (JBTS) and Meckel-Gruber Syndrome (MKS) [56]. Our screen recovered CHD genes that are in each of these three modules. Even more striking is the observation that more than half of the CHD-cilia related genes are also found in the CPLANE (ciliogenesis planar cell polarity) interactome, a PPI network identified by mass spectrometry and shown to regulate ciliogenesis and cilia transduced cell signaling [57]. Given each CHD causing mutation was recovered in entirely independent mutants, the finding of many CHD genes in these cilia related PPI networks would suggest perturbation of these PPI may provide the context for CHD pathogenesis.

To further explore the potential role of an interactome in CHD pathogenesis, we used the 61 CHD genes recovered in our screen to nucleate the assembly of a PPI network comprising known and predicted PPI. This assembly yielded a network of 778 genes, 292 of which are predicted PPIs (Fig. 8). The average shortest distance between CHD genes is 4.3 ± 2.5 edges vs. 5.7 ± 4.4 edges ($P = 0.01$) for random genes of matched degree distribution. These findings suggest a PPI network may provide a rich context to explore the genetic etiology of CHD. In this context, heterozygous mutations in multiple genes in the CHD interactome could cause functional disruption in the network that may lead to CHD. This could account for the fact that mutations causing human CHD are largely heterozygous and often associated with incomplete penetrance and variable expressivity. The latter could reflect the varying combinations of mutations contributing to disease.

12. Clinical translational relevance

The realization of the potential importance of cilia mutations in CHD, especially associated with heterotaxy, has led us to explore the idea that CHD patients may have increased risk for respiratory cilia

Table 3
Functional annotation of de novo mutations in PCGC patients.
Adapted from Li et al. Nature 2015 [21].

Patient ID	CHD§	Gene	Mutation	Gene function
1-00638	CTD	FBN2	p.D2191N	TGFβ signaling
1-02020	HTX	SMAD2	p.IVS12+1G>A	TGFβ signaling
1-02621	HTX	SMAD2	p.W244C	TGFβ signaling
1-00197	LVO	BCL9	p.M1395K	WNT signaling
1-01828	CTD	DAPK3	p.P193L	WNT signaling
1-01138	LVO	USP34	p.L432P	WNT signaling
1-00802	LVO	PTCH1	p.R831Q	SHH signaling/ciliome
1-02598	HTX	LRP2[a]	p.E4372K	SHH signaling/endocytic trafficking
1-01913	Other	RAB10	p.N112S	Endocytic trafficking
1-00750	LVO	HUWE1	p.R3219C	Ciliome
1-01151	CTD	SUV420H1	p.R143C	Ciliome
1-00853	CTD	WDR5	p.K7Q	Ciliome
1-02952	LVO	PITX2	p.A47V	Laterality related

[a]LRP2 is an endocytic gene also recovered from our mouse screen. §CTD: conotruncal defect; HTX: heterotaxy; LVO: left ventricular obstruction.
Lines are colored based on gene function and genes with similar function are highlighted in the same color.

dysfunction [58–60]. In fact, respiratory complications are the major cause for increased morbidity and mortality after congenital cardiac surgeries [61]. While this is generally attributed as secondary to the structural heart disease, the underlying cause remains largely unexplained. Rather studies we have conducted examining cilia motility from nasal epithelia obtained using nasal scrapes have revealed a high prevalence of motile cilia dysfunction in CHD patients [60]. Thus, high speed/high resolution videomicroscopy examination of the ciliated nasal epithelia have shown abnormal ciliary motion in > 30% of CHD patients [60]. Given the fact that mutations causing PCD can give rise to CHD in conjunction with heterotaxy, a compelling question was whether CHD-heterotaxy patients with airway ciliary dysfunction might have undiagnosed PCD. Interestingly, analysis of such a CHD-heterotaxy patient cohort with whole exome sequencing analysis did identify one patient with ciliary dysfunction carrying a pathogenic *DNAI1* mutation known to cause PCD [60]. However, as this mutation was found only in heterozygosity, it is not consistent with the diagnosis of PCD, which is a recessive disorder.

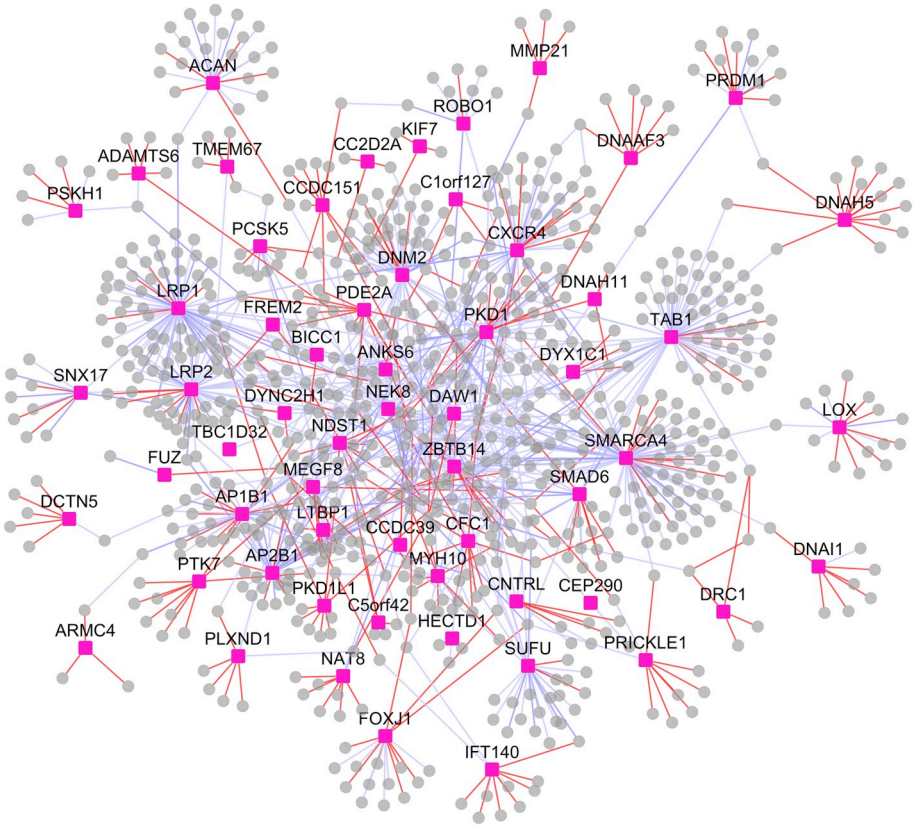

Fig. 8. Protein-Protein interaction network of CHD genes.
An interactome network was constructed comprising the 61 CHD genes (magenta squares) and their known (blue edges) and predicted (red edges) interactions. (For interpretation of the references to color in this figure legend, the reader is referred to the web version of this article.)
Adapted from Li et al. Nature 2015 [21].

While our first study of ciliary dysfunction in CHD patients focused on heterotaxy patients, we have since confirmed the findings from the previous study with similar observations showing a high prevalence of ciliary dysfunction in non-heterotaxy CHD patients [62]. This included CHD patients with a broad spectrum of lesion types and was focused on older CHD subjects (> 7 years old). This study confirmed CHD patients with ciliary dysfunction have increased PCD related respiratory symptoms and disease [62]. Importantly, another clinical study focused on CHD infants undergoing cardiac surgery in the cardiac intensive care unit further demonstrated increased respiratory complications in CHD infants with respiratory ciliary dysfunction [59,61]. This study showed CHD infants with abnormal respiratory ciliary motion had increased odds of requiring noninvasive positive pressure ventilation (odds ratio = 6.5; 95% CI, 1.5–29.4; P = 0.016) and increased respiratory medication use (OR, 4.4; 95% CI, 1.5–13.3; P = 0.01) [59]. This included the need for albuterol, a finding first observed in studies conducted at Children's National Medical Center for heterotaxy CHD patients [61]. Together these findings suggest respiratory ciliary dysfunction can pose significant risk for postsurgical complications in CHD patients undergoing congenital cardiac surgeries. Hence preoperative screening CHD patients for ciliary dysfunction might provide the opportunity to institute prophylactic airway clearance protocols to reduce respiratory complications and help improve postoperative outcome after congenital cardiac surgery. These findings show the potential for basic science discoveries to impact the clinical management of patient care. Such practical clinical translational application of basic discoveries can potentially improve the outcome for CHD patients.

Declaration of Competing Interest

George C. Gabriel, No conflict of interest.
Cecilia W. Lo, No conflict of interest.

Acknowledgements

This work was supported by NIH grants HL132024 and HL142788 (CWL) and 1F30HD097967 (GCG).

References

[1] Liu Y, Chen S, Zuhlke L, Black GC, Choy MK, Li N, et al. Global birth prevalence of congenital heart defects 1970-2017: updated systematic review and meta-analysis of 260 studies. Int J Epidemiol 2019;48(2):455–63.
[2] van der Linde D, Konings EE, Slager MA, Witsenburg M, Helbing WA, Takkenberg JJ, et al. Birth prevalence of congenital heart disease worldwide: a systematic review and meta-analysis. J Am Coll Cardiol 2011;58:2241–7.
[3] Fahed AC, Gelb BD, Seidman JG, Seidman CE. Genetics of congenital heart disease: the glass half empty. Circ Res 2013;112:707–20.
[4] Benson DW, Sharkey A, Fatkin D, Lang P, Basson CT, McDonough B, et al. Reduced penetrance, variable expressivity, and genetic heterogeneity of familial atrial septal defects. Circulation 1998;97:2043–8.
[5] Prendiville T, Jay PY, Pu WT. Insights into the genetic structure of congenital heart disease from human and murine studies on monogenic disorders. Cold Spring Harb Perspect Med 2014;4.
[6] Kirk EP, Sunde M, Costa MW, Rankin SA, Wolstein O, Castro ML, et al. Mutations in cardiac T-box factor gene TBX20 are associated with diverse cardiac pathologies, including defects of septation and valvulogenesis and cardiomyopathy. Am J Hum Genet 2007;81:280–91.
[7] Jin SC, Homsy J, Zaidi S, Lu Q, Morton S, DePalma SR, et al. Contribution of rare inherited and de novo variants in 2,871 congenital heart disease probands. Nat Genet 2017;49:1593–601.
[8] Hoang TT, Goldmuntz E, Roberts AE, Chung WK, Kline JK, Deanfield JE, et al. The congenital heart disease genetic network study: cohort description. PLoS One 2018;13:e0191319.
[9] Pasipoularides A. The new era of whole-exome sequencing in congenital heart disease: brand-new insights into rare pathogenic variants. J Thorac Dis 2018;10:S1923–9.
[10] Mouse Genome Sequencing C, Waterston RH, Lindblad-Toh K, Birney E, Rogers J, Abril JF, et al. Initial sequencing and comparative analysis of the mouse genome. Nature 2002;420:520–62.
[11] Rosenthal N, Brown S. The mouse ascending: perspectives for human-disease models. Nat Cell Biol 2007;9:993–9.
[12] Wessels A, Sedmera D. Developmental anatomy of the heart: a tale of mice and man. Physiol Genomics 2003;15:165–76.
[13] Moon A. Mouse models of congenital cardiovascular disease. Curr Top Dev Biol 2008;84:171–248.
[14] Stanford WL, Cohn JB, Cordes SP. Gene-trap mutagenesis: past, present and beyond. Nat Rev Genet 2001;2:756–68.
[15] Carlson CM, Dupuy AJ, Fritz S, Roberg-Perez KJ, Fletcher CF, Largaespada DA. Transposon mutagenesis of the mouse germline. Genetics 2003;165:243–56.
[16] Horie K, Yusa K, Yae K, Odajima J, Fischer SE, Keng VW, et al. Characterization of Sleeping Beauty transposition and its application to genetic screening in mice. Mol Cell Biol 2003;23:9189–207.
[17] Justice MJ, Noveroske JK, Weber JS, Zheng B, Bradley A. Mouse ENU mutagenesis. Hum Mol Genet 1999;8:1955–63.
[18] Siepka SM, Yoo SH, Park J, Song W, Kumar V, Hu Y, et al. Circadian mutant Overtime reveals F-box protein FBXL3 regulation of cryptochrome and period gene expression. Cell 2007;129:1011–23.
[19] Beutler B. Innate immunity and the new forward genetics. Best Pract Res Clin Haematol 2016;29:379–87.
[20] Hoebe K, Beutler B. Forward genetic analysis of TLR-signaling pathways: an evaluation. Adv Drug Deliv Rev 2008;60:824–9.
[21] Li Y, Klena NT, Gabriel GC, Liu X, Kim AJ, Lemke K, et al. Global genetic analysis in mice unveils central role for cilia in congenital heart disease. Nature 2015;521:520–4.
[22] Liu X, Kim AJ, Reynolds W, Wu Y, Lo CW. Phenotyping cardiac and structural birth defects in fetal and newborn mice. Birth Defects Res 2017;109:778–90.
[23] Liu X, Francis R, Kim AJ, Ramirez R, Chen G, Subramanian R, et al. Interrogating congenital heart defects with noninvasive fetal echocardiography in a mouse forward genetic screen. Circ Cardiovasc Imaging 2014;7:31–42.
[24] Shen Y, Leatherbury L, Rosenthal J, Yu Q, Pappas MA, Wessels A, et al. Cardiovascular phenotyping of fetal mice by noninvasive high-frequency ultrasound facilitates recovery of ENU-induced mutations causing congenital cardiac and extracardiac defects. Physiol Genomics 2005;24:23–36.
[25] Liu X, Yagi H, Saeed S, Bais AS, Gabriel GC, Chen Z, et al. The complex genetics of hypoplastic left heart syndrome. Nat Genet 2017;49:1152–9.
[26] Gordon BM, Rodriguez S, Lee M, Chang RK. Decreasing number of deaths of infants with hypoplastic left heart syndrome. J Pediatr 2008;153:354–8.
[27] Reller MD, Strickland MJ, Riehle-Colarusso T, Mahle WT, Correa A. Prevalence of congenital heart defects in metropolitan Atlanta, 1998–2005. J Pediatr 2008;153:807–13.
[28] Berg C, Geipel A, Smrcek J, Krapp M, Germer U, Kohl T, et al. Prenatal diagnosis of cardiosplenic syndromes: a 10-year experience. Ultrasound Obstet Gynecol 2003;22:451–9.
[29] Taketazu M, Lougheed J, Yoo SJ, Lim JS, Hornberger LK. Spectrum of cardiovascular disease, accuracy of diagnosis, and outcome in fetal heterotaxy syndrome. Am J Cardiol 2006;97:720–4.
[30] Pepes S, Zidere V, Allan LD. Prenatal diagnosis of left atrial isomerism. Heart 2009;95:1974–7.
[31] Atkinson DE, Drant S. Diagnosis of heterotaxy syndrome by fetal echocardiography. Am J Cardiol 1998;82(1147–1149):A1110.
[32] Friedberg MK, Silverman NH, Moon-Grady AJ, Tong E, Nourse J, Sorenson B, et al. Prenatal detection of congenital heart disease. J Pediatr 2009;155(31):26–31. [e21].
[33] Dasgupta A, Amack JD. Cilia in vertebrate left-right patterning. Philos Trans R Soc Lond B Biol Sci 2016;371.
[34] Mirra V, Werner C, Santamaria F. Primary ciliary dyskinesia: an update on clinical aspects, genetics, diagnosis, and future treatment strategies. Front Pediatr 2017;5:135.
[35] Tan SY, Rosenthal J, Zhao XQ, Francis RJ, Chatterjee B, Sabol SL, et al. Heterotaxy and complex structural heart defects in a mutant mouse model of primary ciliary dyskinesia. J Clin Invest 2007;117:3742–52.
[36] Kim AJ, Francis R, Liu X, Devine WA, Ramirez R, Anderton SJ, et al. Microcomputed tomography provides high accuracy congenital heart disease diagnosis in neonatal and fetal mice. Circ Cardiovasc Imaging 2013;6:551–9.
[37] Kennedy MP, Omran H, Leigh MW, Dell S, Morgan L, Molina PL, et al. Congenital heart disease and other heterotaxic defects in a large cohort of patients with primary ciliary dyskinesia. Circulation 2007;115:2814–21.
[38] Shapiro AJ, Davis SD, Ferkol T, Dell SD, Rosenfeld M, Olivier KN, et al. Laterality defects other than situs inversus totalis in primary ciliary dyskinesia: insights into situs ambiguus and heterotaxy. Chest 2014;146:1176–86.
[39] Waters AM, Beales PL. Ciliopathies: an expanding disease spectrum. Pediatr Nephrol 2011;26:1039–56.
[40] Czarnecki PG, Gabriel GC, Manning DK, Sergeev M, Lemke K, Klena NT, et al. ANKS6 is the critical activator of NEK8 kinase in embryonic situs determination and organ patterning. Nat Commun 2015;6:6023.
[41] Damerla RR, Cui C, Gabriel GC, Liu X, Craige B, Gibbs BC, et al. Novel Jbts17 mutant mouse model of Joubert syndrome with cilia transition zone defects and cerebellar and other ciliopathy related anomalies. Hum Mol Genet 2015;24:3994–4005.
[42] Srour M, Schwartzentruber J, Hamdan FF, Ospina LH, Patry L, Labuda D, et al. Mutations in C5ORF42 cause Joubert syndrome in the French Canadian population. Am J Hum Genet 2012;90:693–700.
[43] Gorden NT, Arts HH, Parisi MA, Coene KL, Letteboer SJ, van Beersum SE, et al. CC2D2A is mutated in Joubert syndrome and interacts with the ciliopathy-associated basal body protein CEP290. Am J Hum Genet 2008;83:559–71.
[44] Kyttala M, Tallila J, Salonen R, Kopra O, Kohlschmidt N, Paavola-Sakki P, et al. MKS1, encoding a component of the flagellar apparatus basal body proteome, is mutated in Meckel syndrome. Nat Genet 2006;38:155–7.

[45] Hartill V, Szymanska K, Sharif SM, Wheway G, Johnson CA. Meckel-Gruber Syndrome: an update on diagnosis, clinical management, and research advances. Front Pediatr 2017;5:244.
[46] Barisic I, Boban L, Loane M, Garne E, Wellesley D, Calzolari E, et al. Meckel-Gruber Syndrome: a population-based study on prevalence, prenatal diagnosis, clinical features, and survival in Europe. Eur J Hum Genet 2015;23:746–52.
[47] Travaglini L, Brancati F, Attie-Bitach T, Audollent S, Bertini E, Kaplan J, et al. Expanding CEP290 mutational spectrum in ciliopathies. Am J Med Genet A 2009;149A:2173–80.
[48] Dyer LA, Kirby ML. Sonic hedgehog maintains proliferation in secondary heart field progenitors and is required for normal arterial pole formation. Dev Biol 2009;330:305–17.
[49] Richarte AM, Mead HB, Tallquist MD. Cooperation between the PDGF receptors in cardiac neural crest cell migration. Dev Biol 2007;306:785–96.
[50] Xu J, Lamouille S, Derynck R. TGF-beta-induced epithelial to mesenchymal transition. Cell Res 2009;19:156–72.
[51] Sung CH, Leroux MR. The roles of evolutionarily conserved functional modules in cilia-related trafficking. Nat Cell Biol 2013;15:1387–97.
[52] Irigoin F, Badano JL. Keeping the balance between proliferation and differentiation: the primary cilium. Curr Genomics 2011;12:285–97.
[53] Zaidi S, Choi M, Wakimoto H, Ma L, Jiang J, Overton JD, et al. De novo mutations in histone-modifying genes in congenital heart disease. Nature 2013;498:220–3.
[54] Stagner EE, Bouvrette DJ, Cheng J, Bryda EC. The polycystic kidney disease-related proteins Bicc1 and SamCystin interact. Biochem Biophys Res Commun 2009;383:16–21.
[55] Habbig S, Bartram MP, Sagmuller JG, Griessmann A, Franke M, Muller RU, et al. The ciliopathy disease protein NPHP9 promotes nuclear delivery and activation of the oncogenic transcriptional regulator TAZ. Hum Mol Genet 2012;21:5528–38.
[56] Sang L, Miller JJ, Corbit KC, Giles RH, Brauer MJ, Otto EA, et al. Mapping the NPHP-JBTS-MKS protein network reveals ciliopathy disease genes and pathways. Cell 2011;145:513–28.
[57] Toriyama M, Lee C, Taylor SP, Duran I, Cohn DH, Bruel AL, et al. The ciliopathy-associated CPLANE proteins direct basal body recruitment of intraflagellar transport machinery. Nat Genet 2016;48:648–56.
[58] Zahid M, Bais A, Tian X, Devine W, Lee DM, Yau C, et al. Airway ciliary dysfunction and respiratory symptoms in patients with transposition of the great arteries. PLoS One 2018;13:e0191605.
[59] Stewart E, Adams PS, Tian X, Khalifa O, Wearden P, Zahid M, et al. Airway ciliary dysfunction: association with adverse postoperative outcomes in nonheterotaxy congenital heart disease patients. J Thorac Cardiovasc Surg 2018;155(755–763):e757.
[60] Nakhleh N, Francis R, Giese RA, Tian X, Li Y, Zariwala MA, et al. High prevalence of respiratory ciliary dysfunction in congenital heart disease patients with heterotaxy. Circulation 2012;125:2232–42.
[61] Harden B, Tian X, Giese R, Nakhleh N, Kureshi S, Francis R, et al. Increased postoperative respiratory complications in heterotaxy congenital heart disease patients with respiratory ciliary dysfunction. J Thorac Cardiovasc Surg 2014;147(1291–1298):e1292.
[62] Garrod AS, Zahid M, Tian X, Francis RJ, Khalifa O, Devine W, et al. Airway ciliary dysfunction and sinopulmonary symptoms in patients with congenital heart disease. Ann Am Thorac Soc 2014;11:1426–32.